Advances in the Development of a Novel Method to be used in Proteomics using Gold Nanobeads

Heidelinde R. C. Dietrich, Ian T. Young and Yuval Garini

Quantitative Imaging Group, Department of Imaging Science & Technology, Faculty of Applied Sciences, Delft University of Technology, Lorentzweg 1, NL-2628 CJ Delft, The Netherlands

ABSTRACT

The study of DNA-protein interactions is gaining increased attention due to their importance in cellular processes. Only a well-functioning interaction guaranties that such a process can take place without errors. So far, only a small percentage of these interactions have been unraveled, partially due to their complexity but also due to the fact that there are only a few techniques that permit the study of these interactions. In this report we describe the development of a research tool based on tethered bead motion and Resonance Light Scattering (RLS) from gold beads. This method permits the study of DNA-protein interactions and the screening of proteins binding to a specific DNA sequence.

Keywords: single molecule detection, resonance light scattering, molecular interactions, quantitative microscopy

1. INTRODUCTION

DNA replication[1,2], DNA repair, transcription and many other cellular processes are the result of a complex network between various biological components. Motor proteins, for instance, bind to other molecules and regulate their function. Proteins that bind to double and single stranded DNA, so called DNA-binding proteins, fulfill essential functions such as the regulation of genes. Only a small percentage of protein interactions and their individual mechanisms have been investigated leaving an enormous number waiting to be unraveled.

The study[1,2,3] of the interaction of proteins with DNA (double or single stranded) covers a broad range of research and includes, the screening of DNA-binding proteins, the identification of a DNA recognition sequence, the analysis of binding affinities between protein and DNA, and the investigation of DNA binding events controlling specific tasks like gene expression. There are a number[1,2] of different methods for the analysis of DNA-protein interactions such as DNA footprinting, electrophoretic mobility shift assays (EMSA), and DNA-protein photocrosslinking, These are standard methods for DNA-protein interaction research. Today, this palette has been broadened by other methods that make use of special devices like DNA-microarrays[4] or that are based on phenomena like surface plasmon resonance (SPR) [5,6]. However, all these techniques have one weakness. They deal with a large population of molecules and the analyzed data are averaged over this large group of molecules. This does not always permit the understanding of individual molecular mechanisms. In the last ten to twenty years, single-molecule techniques (SMT)[7,8] have become more advanced and new techniques have been developed. These techniques permit the study of molecular mechanisms in a number of different measurements at the single molecule level. Molecular motors[8] like kinesin and myosin have been studied by means of optical tweezers, magnetic tweezers and total internal reflection fluorescence microscopy (TIRFM). Other methods that are used in biomechanical studies are scanning probe microscopy (SPM), microneedle, near-field scanning optical microscopy (NSOM), fluorescence resonance energy transfer (FRET), fluorescence correlation spectroscopy (FCS), surface enhanced Raman spectroscopy (SERS), and tethered bead motion (TPM) also called single particle tracking (SPT). Optical and magnetic tweezers and microneedles are not only capable of detecting single molecules but of manipulating biomolecules.

2. METHOD

The single-molecule detection method we are developing is based on tethered particle motion (TPM). In TPM[9,10,11], one end of a biopolymer (e.g. DNA, RNA) is immobilized onto a glass slide. The other end of the molecule is labeled with a micro- or nanometer scale bead. The position of this sphere in solution is limited within a volume that depends on the length of the biopolymer. A precise determination of this volume allows the prediction of the length of the immobilized

Ultrasensitive and Single-Molecule Detection Technologies, edited by Jörg Enderlein, Zygmunt K. Gryczynski, Proc. of SPIE Vol. 6092, 60920C, (2006) · 1605-7422/06/$15 · doi: 10.1117/12.645908

biopolymer and possible variations in its length due to interaction with other molecules (e.g. proteins) or due to differences in its environment caused by changing the pH, salt concentration, etc (Figure 1).

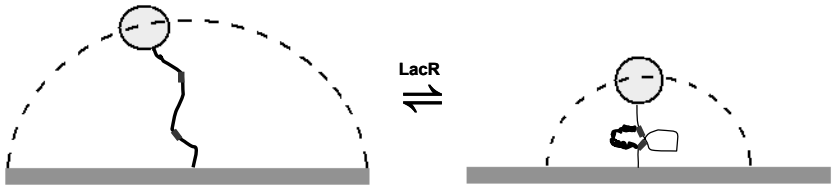

Figure 1. The Lactose repressor protein is binding to two *lac* operators on a dsDNA. This protein shortens the DNA strand by inducing a loop, which decreases the length of the DNA and consequently the range of movement within a certain volume.

Schafer *et al*. (1991) were the first to report on this method. They were studying the kinetics of *E.coli* RNA polymerase. Finzi *et al*. (1995) measured DNA looping by the lactose repressor protein of *E.coli* in single fragments of double-stranded DNA. More research publications followed that not only reported on the use of TPM in connection with video-microscopy in order to study biomolecular interactions but also on the analysis of the resulting data utilizing the TPM method[12,13,14,15].

Our method[16] makes use of gold beads (∅ ≈ 80 nm) in contrast to the polystyrene beads usually used in TPM. These metallic beads differentially scatter polychromatic light depending on the bead size and the plasmon-photon interaction[17]. We use gold beads (RLS beads, Invitrogen, The Netherlands) that are commonly tagged with anti-biotin antibodies. The DNA fragments were amplified from a lambda DNA template using the Expand Long Template PCR System (Roche) and are modified with a thiol group and a biotin. Each double-stranded DNA fragment (≈5 kb) is labeled with a single metallic bead and tethered on a gold substrate (Figure 2) via the thiol linkage. The anti-biotin labeled RLS beads bind to the free biotin on the dsDNA.

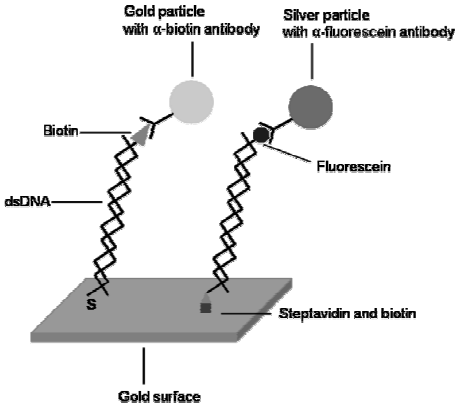

Figure 2. Double-stranded DNA fragments labeled with gold and silver beads immobilized on a gold surface.

We use a darkfield microscopy (Olympus BX51) with a 20x/0.46 objective in order to detect the scattered light of the gold beads. The motion of the beads is monitored by means of a 12 bit CCD camera (Hamamatsu, Orca-ER C4742-95). The CCD array consists of 1344 x 1024 pixels. Each pixel has a size of 6.45 µm x 6.45 µm. The CCD camera is controlled by SimplePCI from Compix Inc. Imaging Systems. The sampling density in x- and y- directions are: $\Delta_x = 0.327$ µm (3.06

samples per μm) and Δ_y = 0.322 μm (3.11 samples per μm), just under the Nyquist frequency. The collected images are analyzed by MATLAB using our in-house software package DIP Image[18].

3. RESULTS AND DISCUSSION

Our results are based on the detection of the constrained motion of dsDNA fragments tagged with gold nanospheres The evaluation of the data was done from the standpoint of kinetic theory and diffusion.

Some experiments were performed at a frame rate of ≈33 frames per second (30 ms exposure time) and some at 25 frames per second (40 ms exposure time). Experiments were performed at ambient temperature. A TRIS/EDTA (10 mM/1 mM) buffer pH 8 was used. We monitor the motion of the bead for at least 5 minutes in order to get a more accurate estimation of the dynamics of its movement. The dsDNA fragments used in all experiments were 4861 bp long. The term "fixed bead" refers to a gold nanobead that is directly immobilized on the gold surface of the chip due to non-specific interactions. Fixed beads are reference points for drift correction and noise estimation. Moving beads are the ones that are tethered to the gold support via the dsDNA fragment. These beads are mobile and show constrained motion within a volume which is depends upon the length of the DNA fragment. All data fits were performed using the Solver function of Microsoft Excel.

The average and root-mean-square values of the change in position, $\Delta r = \sqrt{(\Delta x)^2 + (\Delta y)^2}$, for a fixed bead and a moving bead are shown in Table 1. The changes, Δx and Δy, are derived from (x, y) coordinate measurements of the center-of-mass of the bead image in two subsequent image frames separated by 30 ms or 40 ms. The average value of Δr and the rms value of Δr for a fixed bead are a factor of about 50 smaller compared to that of a moving bead. The fact that stationary beads show any movement at all is due to noise in the entire measurement system – mechanical vibrations, camera noise, etc. In general, data from fixed beads provide control values that can be regarded as the error of the method and system respectively.

Table 1. Average and rms of Δr for a fixed bead and a moving bead.

	Fixed [nm]	**Moving [nm]**
$< \Delta r >$	2.71	135
$\sqrt{< \Delta r^2 >}$	3.12	155

The radial positions of a tethered, moving bead are shown in Figure 3a. The collection of (x, y) coordinates, N = 5000, show no preferential direction. The histogram of the radii of theses 5000 points is shown in Figure 3b.

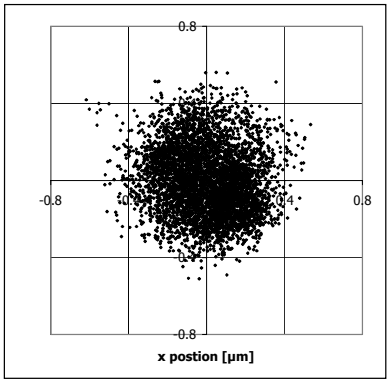

(a) Position at each time point Δt = 30 ms.

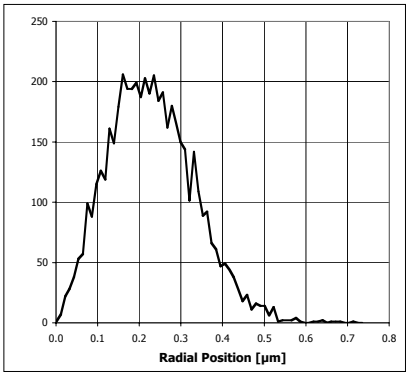

(b) Histogram of radial distances

Figure 3. Analysis of 5000 (x, y) coordinates of a moving bead attached to tethered DNA.

Looking at Figure 3 we realize that the extent of the bead motion seems to be too small. The average radial distance is 225 nm. The 99% maximum radius—taken from the histogram—is 491 nm. But the "length" of a 4681 bp dsDNA fragment is about 1591 nm. This means that the measured fragment should give a maximum radial distance of 1591 nm, which is 7 times larger than the average value of r and 3.2 times larger than the maximum we found. A possible explanation is as follows. Double-stranded DNA is not a very rigid molecule. Its persistence length[19] is about 50 nm under conditions comparable to the ones described here. It is, therefore, unlikely that the tethered dsDNA will be stretched to its theoretical end-to-end distance of 1591 nm.

We have calculated the most likely length of the radius of gyration of a 4681 bp dsDNA fragment which is 280 nm (data not shown), a value that is similar to the expected end-to-end distance[20].

The average changes in the *magnitude* of movement in the x and y directions are given in Table 2. As could be expected, the average changes in $|\Delta x|$ and $|\Delta y|$ for a fixed bead are considerably smaller than those of a moving one. This values for a fixed bead can, again, be taken as a control value for noise. The small average changes in the x and y directions for a moving bead are striking. They imply that the bead moves in very small steps rather than jumping from one site to another. This indicates as well that the integration time of the camera and the frame rate of the experiments are satisfactory. Temporal aliasing can, therefore, be excluded.

Table 2. Average magnitude changes in x- and y-direction for a fixed and moving bead.

	Fixed [nm]	**Moving [nm]**
$<\|\Delta x\|>$	1.39	87.90
$<\|\Delta y\|>$	2.78	84.14

Table 3 depicts the average speed of a fixed and moving bead. The stationary bead shows an average speed of 0.048 nm per second. This is about 40 times smaller than a bead in motion. The fact that this fixed point gives a value other than zero can be referred to as a noise figure for the entire detection platform.

The 2D root-mean-square velocities of the moving bead, given in Table 3, is about 65 times larger than the non-moving one. The equipartition theorem permits a simple estimation of the 3D velocities given the 2D velocities. These values point out that a clear difference between stationary and moving beads can be made.

Table 3. Average speed for a fixed bead and a moving bead.

	Fixed [nm/s] **$\Delta t = 40$ ms**	**Moving [nm/s]** **$\Delta t = 30$ ms**
average speed	.048	1.90
$\sqrt{<v^2>}$ **(2D)**	80	5170
$\sqrt{<v^2>}$ **(3D)**	120	7760

From kinetic theory, the velocity of a completely free bead whose movement is caused by Brownian motion can be described by a Maxwell-Boltzmann distribution:

$$f(v) = A \bullet v^2 \bullet e^{-\alpha v^2} \tag{1}$$

A and α are fitting parameters and v^2 corresponds to the length-squared of the velocity vector. The resulting fit to the data is shown in Figure 4. The value of α that is determined by the fitting procedure can provide an estimate of an "effective" mass. This value is given by $m_{MB} = 2 \bullet \alpha \bullet kT$ where k is the Boltzmann constant and T is the ambient temperature in Kelvin (300 K). Using the value found for α in Figure 4, $\alpha = 0.063$, gives a mass estimate of $m_{MB} = 5.22 \times 10^{-7}$ fg.

But from kinetic theory, the equivalent mass m of a bead whose movement is caused by Brownian motion can also be calculated from:

$$m = \frac{3kT}{< v^2 >} \tag{2}$$

where $<v^2>$ is the mean-square velocity. The calculated equivalent mass of the moving bead can be calculated and the resulting value for the dsDNA, 80 nm tethered bead is 2.06×10^{-7} fg. This value is close to the value from the Maxwell-Boltzmann fit and that should be no surprise. The factor of 2.5 difference can be attributed to the smoothing effect associated with the fitting of the Maxwell-Boltzmann curve. Both of these values, however, are far less than the weight of the gold bead which is 4.14×10^{-2} fg indicating that a simple Maxwell-Boltzmann model is not sufficient to describe the motion of this tethered gold bead.

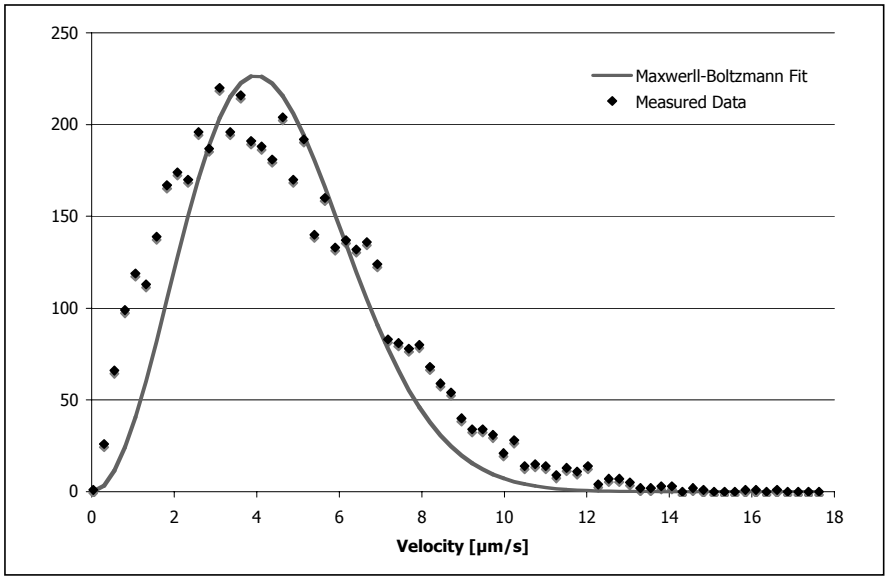

Figure 4. Maxwell-Boltzmann distribution of a moving bead. Fitted values are $a = 0.063$ and $A = 38.82$

The movement can also be characterized by the diffusion coefficient of a bead. The experimental diffusion coefficients were calculated according to the following equation:

$$D = \frac{\Delta t < v^2 >}{2n} \tag{3}$$

where Δt is the time between two frames and n corresponds to the number of observed spatial dimensions. Figure 5 depicts the experimental diffusion coefficients for free beads (free in solution), tethered beads (constrained movement) and fixed beads.

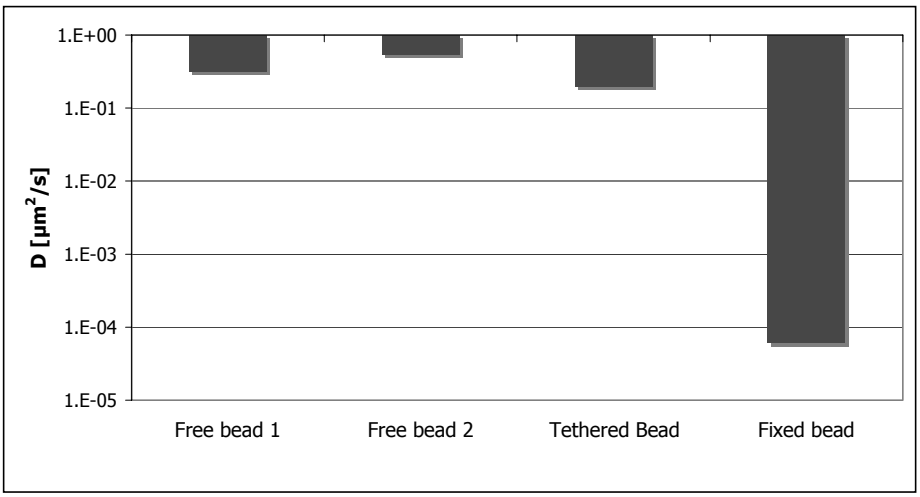

Figure 5. Measured diffusion coefficients. Note the logarithmic vertical scale.

Free beads diffuse about 2 times faster than beads that are tethered and thus constrained to move within a certain volume. Both can be clearly distinguished from two beads that are fixed to the chip surface and give a diffusion coefficient more than 3000 times smaller than free and tethered spheres.

The angular change as a tethered bead moves from one frame time to another can also be measured. Figures 6 and 7 show the distribution of the change in angle, $\Delta\theta$, of a fixed and moving bead. Both distributions can be well described by a bi-exponential function. The following equation was used to fit the data:

$$f(\Delta\theta) = Be^{-\beta(\Delta\theta-\theta_o)} \tag{4}$$

where $\Delta\theta$ is the change in angle from one frame to another and B, β, and θ_o are fitting parameters.

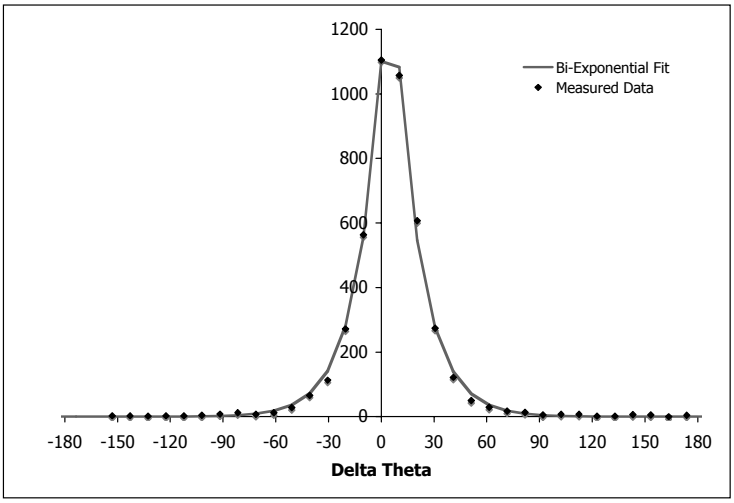

Figure 6. Distribution of $\Delta\theta$ of a fixed bead. Fitted values are B = 1536.5, β = 0.067, and θ_o = 5.06.

The fits shown in Figures 6 and 7 are extremely good. We do not have at this time a model that predicts this distribution. Investigations will, of course, continue.

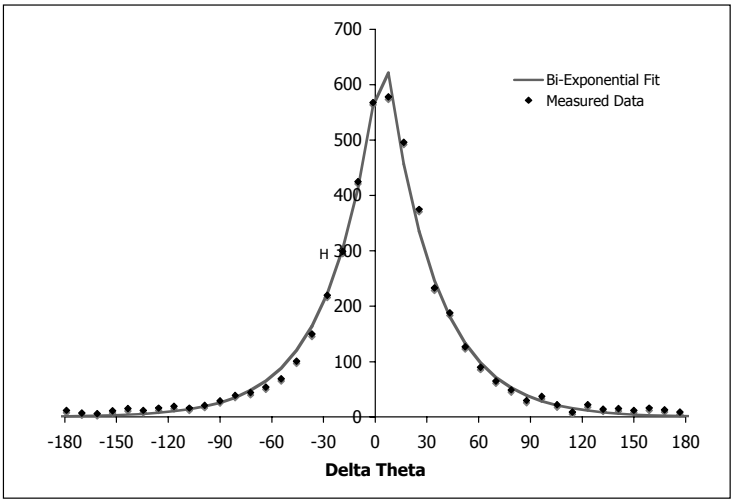

Figure 7. Distribution of $\Delta\theta$ of a moving bead. Fitted values are $B = 689.5$, $\beta = 0.035$, and $\theta_o = 4.72$.

4. CONCLUSIONS

We are able to follow the motion of 80 nm gold beads tethered to a gold support by using a 4862 bp long dsDNA fragment. These beads can be distinguished from beads that are directly immobilized onto the gold surface by means of kinetic theory and diffusion.

The average radius of a moving bead (tethered to dsDNA) does not reach the "theoretical" value which depends on the contour length of the DNA fragment. This is due to the fact that DNA is not a stiff polymer but has a rather flexible structure. Only when an external force is applied to the DNA can the fragment be extended to its maximum end-to-end distance[21]. In order to make a prediction on the distribution of the bead's position and motion in solution, we will be examining the details of the physics of a DNA fragment tethered on a solid support.

ACKNOWLEDGEMENTS

We thank Wim van Oel and Guus Liqui Lung for their help in technical matters. We thank Prof. Theo Odijk for many valuable discussions and his calculation of the DNA radius of gyration. This work was partially supported by the Bsik Research Program *Cyttron* and the Delft Research Center *Life Science and Technology*

REFERENCES

1 M. J. Guille, G. G. Kneale, "Methods for the Analysis of DNA-Protein Interactions", Mol. Biotechnol. 8, pp. 35-52, 1997.

2 J. S. Shumaker-Parry *et al.*, "Probing Protein-Interactions Using a Uniform Monolayer of DNA and Surface Plasmon Resonance", Scanning and Force Microscopies for Biomedical Applications II, E. Tamiya and E. S. Yeung ed., Proceedings of SPIE 3922, pp. 1605-7422, 2000.

3 M. Berezovski, S. N. Krylov, "Using DNA-Binding Proteins as an Analytical Tool", JACS 125 (44), pp. 13451-13454, 2003.

4 B. Ren *et al.*, "Genome-Wide Location and Function of DNA-Binding Proteins", Science 290, pp. 2306-2309, 2000.

5 F. Schubert *et al*., "Comparative Thermodynamic Analysis of DNA-Protein Interactions Using Surface Plasmon Resonance and Fluorescence Correlation Spectroscopy", Biochemistry 42, pp. 10288-10294, 2003.

6 P. Y. Tsoi, M. Yang, "Surface plasmon resonance study of the molecular recognition between polymerase and DNA containing various mismatches and conformational changes of DNA-protein complexes", Biosens. Bioelectron. 19, pp. 1209-1218.

7 R. Brown *et al*., "Review of Techniques for Single Molecule Detection in Biological Applications", NPL Report COAM 2, National Physical Laboratory, Queens Road, Teddington, Middlesex, TW1 0LW, September 2001.

8 Y. Ishii, T Yanagida, "Single Molecule Detection in Life Science", Single Mol. 1, pp. 5-16, 2000.

9 M. Capitanio *et al*., " Exploring Molecular Motors and Switches at the Single-Molecule Level", Microsc. Res. Tech. 65, pp. 194-204, 2004.

10 H. Qian *et al*., "Single particle tracking", Biophys. J. 60, pp. 910-921, 1991.

11 N. Pouget *et al.*, "Single-particle tracking for DNA tether length monitoring", Nucleic Acids Res. 32 (9): e73, 2004.

12 H. Qian, E. L. Elson, "Quantitative Study of Polymer Conformation and Dynamics by Single-Particle Tracking", Biophys. J. 76, pp. 1598-1605, 1999.

13 H. Qian, "A mathematical analysis for the Brownian dynamics of a DNA tether", J. Math. Biol. 41, pp. 331-340, 2000.

14 K. M. Dohoney, J. Gelles, "χ-Sequence recognition and DNA translocation by single RecBCD helicase/nuclease molecules", Nature 409, pp. 370-374, 2001.

15 F. Vanzi *et al*., "Protein synthesis by single ribosomes", RNA 9, pp. 1174-1179, 2003.

16 H. R. C. Dietrich *et al*., "Gold nanoparticles: A Novel Application of Spectral Imaging in Proteomics - Preliminary Results, Spectral Imaging: Instrumentation, Applications, and Analysis III (Proc. Conf. San Jose, CA, USA, Jan. 22-27), Proc. SPIE, vol. 5694, 2005, 82-89.

17 J. Yguerabide, E. E. Yguerabide, "Light-Scattering Submicroscopic Particles as Highly Fluorescent Analogs and Their Use as Tracer Labels in Clinical and Biological Applications", Anal. Biochem. 262, pp. 137–156, 1998.

18 C. Luengo Hendriks *et al.*, DIPimage: a scientific image processing toolbox for MATLAB. Delft University of Technology, http://www.qi.tnw.tudelft.nl/DIPlib.

19 V. A. Bloomfield *et al.*, "Nucleic Acids: Structures, Properties, Functions", University Science Press, New York, 2000.

20 T. Odijk, "On the Ionic-Strength Dependence of the Intrinsic Viscosity of DNA", Biopolymers 18, pp. 3111-3113, 1979.

21 C. Bustamante *et al.*, "Ten years of tension: single-molecule DNA mechanics", Nature 421, pp. 423-427, 2003.